Computer Vision and Image Understanding 117 (2013) 429–437

Contents lists available at SciVerse ScienceDirect

Computer Vision and Image Understanding

journal homepage: www.elsevier.com/locate/cviu

The minimum barrier distance

Robin Strand [a,*], Krzysztof Chris Ciesielski [b,c], Filip Malmberg [a], Punam K. Saha [d,e]

[a] Centre for Image Analysis, Uppsala University, Sweden
[b] Department of Mathematics, West Virginia University, Morgantown, WV 26506-6310, USA
[c] Department of Radiology, MIPG, University of Pennsylvania, Blockley Hall – 4th Floor, 423 Guardian Drive, Philadelphia, PA 19104-6021, USA
[d] Department of Electrical and Computer Engineering, The University of Iowa, Iowa City, IA 52242, USA
[e] Department of Radiology, The University of Iowa, Iowa City, IA 52242, USA

ARTICLE INFO

Article history:
Received 12 September 2011
Accepted 22 October 2012
Available online 8 December 2012

Keywords:
Image processing
Distance function
Distance transform
Fuzzy subset
Path strength

ABSTRACT

In this paper we introduce a minimum barrier distance, MBD, defined for the (graphs of) real-valued bounded functions f_A, whose domain D is a compact subsets of the Euclidean space $\mathbb{R}^n$. The formulation of MBD is presented in the continuous setting, where D is a simply connected region in $\mathbb{R}^n$, as well as in the case where D is a digital scene. The MBD is defined as the minimal value of the barrier strength of a path between the points, which constitutes the length of the smallest interval containing all values of f_A along the path.

We present several important properties of MBD, including the theorems: on the equivalence between the MBD ρ_A and its alternative definition φ_A; and on the convergence of their digital versions, $\widehat{\rho_A}$ and $\widehat{\varphi_A}$, to the continuous MBD $\rho_A = \varphi_A$ as we increase a precision of sampling. This last result provides an estimation of the discrepancy between the value of $\widehat{\rho_A}$ and of its approximation $\widehat{\varphi_A}$. An efficient computational solution for the approximation $\widehat{\varphi_A}$ of $\widehat{\rho_A}$ is presented. We experimentally investigate the robustness of MBD to noise and blur, as well as its stability with respect to the change of a position of points within the same object (or its background). These experiments are used to compare MBD with other distance functions: fuzzy distance, geodesic distance, and max-arc distance. A favorable outcome for MBD of this comparison suggests that the proposed minimum barrier distance is potentially useful in different imaging tasks, such as image segmentation.

1. Introduction

Over the past several decades, distance transform (DT) [1–7] has been widely used as an effective tool for analyzing object morphology and geometry [8–10]. Most DT measures described in the literature essentially capture the Euclidean distance of a candidate point from a target set, often the background. Rosenfeld and Pfaltz [11] introduced the simple yet fundamental idea that, in a digital grid, the global Euclidean distance transform may be approximated by propagating local distances between neighboring pixels. Borgefors [2,3] extensively studied DTs for binary objects including the popular algorithm [2] that computes DT by using different local step lengths for different types of neighbors. Also, she studied the geometry and equations of 3D DT and presented a two-pass raster scan algorithm for computing approximate Euclidean distance transform [3]. An algorithm for computing in linear time the exact Euclidean distance transform for the rectangular digital images was described in [12] and elaborated on in [13].

Other authors have considered distance functions where the image data is taken into account, see, e.g., [5,14–16]. Distance transforms for such distance functions are typically computed on discrete sets using variations on Dijkstra's algorithm. Falcão et al. showed that this method of computation can be used for any *smooth* distance function, as defined in [16].

Image processing on fuzzy subsets has gained a lot attention, [9,10,17,18]. It provides a flexible framework for handling uncertainty, arising from sampling artifacts, illumination inhomogeneities and other imperfections in the image representation and acquisition process. Fuzzy sets are defined using a membership function which gives the degree of belongingness with respect to some set.

In this paper, we introduce a distance function defined for the real-valued bounded functions f_A (so, in particular, for fuzzy sets), whose domain D is a compact subsets of the Euclidean space $\mathbb{R}^n$. We refer to the new distance as the "minimum barrier distance" and study its properties in the continuous setting, where D is a simply connected region in $\mathbb{R}^n$, as well as in the case where D is a digital scene. In image processing and computer vision, ordinary and fuzzy distance functions [1–6,11,14–16] have widely been used to represent a spatial relation between each pair of points in a Euclidean space or a fuzzy subset. For example, ordinary dis-

* Corresponding author.
E-mail addresses: robin@cb.uu.se (R. Strand), KCies@math.wvu.edu (K.C. Ciesielski), filip@cb.uu.se (F. Malmberg), punam-saha@uiowa.edu (P.K. Saha).

1077-3142/$ - see front matter © 2012 Elsevier Inc. All rights reserved.
http://dx.doi.org/10.1016/j.cviu.2012.10.011

tance function, commonly used for binary images, is a measure of the shortest digital path length between two points while, as viewed by Saha et al. [5], fuzzy distance is a measure of the "minimum material to be traversed" to move from one point to the other where the fuzzy membership function is linked to local material density. Under both ordinary and fuzzy distance frameworks, the length of a path strictly increases as the path grows. The formulation of minimum barrier distance function possesses the following property: The length of a path may remain constant during its growth until a new stronger barrier is met on the path. This subtle shift in the notion of path length allows the new distance function to capture separation between two points in the sense of "connectivity" [19] in a fuzzy set unlike geometric properties commonly represented by existing distance functions. Thus, it may be an interesting avenue to study strengths and limitations of the new function that theoretically behaves like a distance while resembling to "anti-connectivity" from a user perspective. For example, the new distance may be useful to determine minimum barrier to move from one region to another and also, to locate the minimum barrier path. In the context of image processing and computer vision, the new distance function may be useful in image segmentation and region growing.

We show that (pseudo-)metric properties of the "minimum barrier distance" are maintained by its formulation in a digital grid. We give examples that show that the minimum-barrier distance cannot be computed using the standard Dijkstra algorithm mentioned above. Instead, we give an approximation of the new distance measure for fuzzy subsets on digital grids and show that the minimum barrier distance over a continuous fuzzy subset can be approximated arbitrarily close in a digital grid by using a sufficiently dense sampling grid. A similar approximation idea is presented in [20]. An efficient computational solution for the minimum barrier distance is presented using the approximation. The experiments show that the minimum barrier distance is robust to noise, blur, and seed point position.

2. The Minimum Barrier Distance in R^n

Let $f_A : D \to \mathbb{R}$ be any bounded function and let A be its graph, that is,

$$A = \{\langle x, f_A(x)\rangle : x \in D\}.$$

We will concentrate on the functions f_A: $D \to [0,1]$, in which case A will be treated as a fuzzy subset of D and f_A will be referred to as the *membership function* of A in D. However, the presented material works for mappings f_A with any bounded range. For example, $f_A(x)$ could be the intensity value at x in a digital image.

For $D \subset \mathbb{R}^n$ and $p,q \in D$, a *path from p to q* (in D) is any continuous function π: $[0,1] \to D$ with $p = \pi(0)$ and $q = \pi(1)$. We use the symbol $\Pi_{p,q}$ (or just Π, when p and q are clear from the context) to denote the family of all such paths. Recall, that $D \subset \mathbb{R}^n$ is *path connected* provided for every $p,q \in D$ there exists a path π: $[0,1] \to D$ from p to q.

The goal of this section is to introduce and discuss the following notion of the minimum barrier distance defined for the bounded continuous functions $f_A : D \to \mathbb{R}$ in the case when $D \subset \mathbb{R}^n$ is path connected.

Definition 1. For a path π: $[0,1] \to D$, the *barrier* along π is defined as

$$\begin{aligned}\tau_A(\pi) &= \max_t f_A(\pi(t)) - \min_t f_A(\pi(t)) \\ &= \max_{t_0,t_1}(f_A(\pi(t_1)) - f_A(\pi(t_0))).\end{aligned} \tag{1}$$

The *minimum barrier distance* ρ_A: $D \times D \to [0,\infty)$ for a path connected $D \subset \mathbb{R}^n$ is defined via formula

$$\rho_A(p,q) = \inf_{\pi \in \Pi_{p,q}} \tau_A(\pi). \tag{2}$$

Notice that the maxima and minima in the formula (1) are attained (by the Extreme Value Theorem), since the composition function $f_A \circ \pi$ is continuous. At the same time, the next example shows that a path that defines the minimum barrier distance ρ_A is not always attained, that is, the infimum operation in the definition (2) cannot be replaced with the minimum operation.

Example 1. Let $D = [-1,1]^2$ and T be the topologists sine curve, that is, T is the closure of the set $S = \{\langle x, \sin(1/x)\rangle : x \in (0,1]\}$, see Fig. 1. If $f_A(x)$ is defined as the Euclidean distance from $x \in D$ to T, then f_A is continuous. If $p = \langle 0,0\rangle$ and $q = \langle 1, \sin 1\rangle$, then $\inf_{\pi \in \Pi_{p,q}} \tau_A(\pi) = 0$, but $\tau_A(\pi) > 0$ for any $\pi \in \Pi$ (since T is not path connected).

Notice that $\rho_A(p,q)$ is related to the geodesic distance $g_A(p,q)$ between the points $\langle p, f_A(p)\rangle$ and $\langle q, f_A(q)\rangle$ along the surface A. Actually, $\rho_A(p,q)$ is, in a way, a vertical component of $g_A(p,q)$, so that $\rho_A(p,q) \leqslant g_A(p,q)$.

Definition 2. A function d: $D \times D \to [0,\infty)$ is a *metric* on a set D provided, for every $x,y,z \in D$,

(i) $d(x,x) = 0$ (identity)
(ii) $d(x,y) > 0$ for all $x \neq y$ (positivity)
(iii) $d(x,y) = d(y,x)$ (symmetry)
(iv) $d(x,z) \leqslant d(x,y) + d(y,z)$ (triangle inequality)

A function d that obeys properties (i), (iii), and (iv) is called a *pseudo-metric*.

In the proof that ρ_A is a pseudo-metric, we will use the following notion. The *concatenation* $\pi_1 \cdot \pi_2$ of the paths π_1 and π_2 such that $\pi_1(1) = \pi_2(0)$ is

$$(\pi_1 \cdot \pi_2)(t) = \begin{cases} \pi_1(2t) & \text{if } t \in [0, 1/2] \\ \pi_2(2t) & \text{otherwise.} \end{cases}$$

Remark 1. If $\pi_1(1) = \pi_2(0)$, then $\tau_A(\pi_1) + \tau_A(\pi_2) \geqslant \tau_A(\pi_1 \cdot \pi_2)$.

Proposition 1. *ρ_A is a pseudo-metric.*

Proof. It is obvious that ρ_A is non-negative and symmetric. It satisfies the identity property (i), since for the constant path π_x defined via $\pi_x(t) = x$ for all $t \in [0,1]$, we have $\rho_A(x,x) \leqslant \tau_A(\pi_x) = f_A(x) - f_A(x) = 0$.

Now we prove the triangular inequality. Given three arbitrary points $p,q,r \in D$ and an $\varepsilon > 0$ chose the paths $\pi_{p,q} \in \Pi_{p,q}$ and $\pi_{q,r} \in \Pi_{q,r}$ such that $\rho_A(p,q) \geqslant \tau(\pi_{p,q}) - \varepsilon$ and $\rho_A(q,r) \geqslant \tau(\pi_{q,r}) - \varepsilon$. Then, using Remark 1, we have

$$\begin{aligned}\rho_A(p,q) + \rho_A(q,r) &\geqslant \tau(\pi_{p,q}) - \varepsilon + \tau(\pi_{q,r}) - \varepsilon \geqslant \tau_A(\pi_{p,q} \cdot \pi_{q,r}) - 2\varepsilon \\ &\geqslant \rho_A(p,r) - 2\varepsilon.\end{aligned}$$

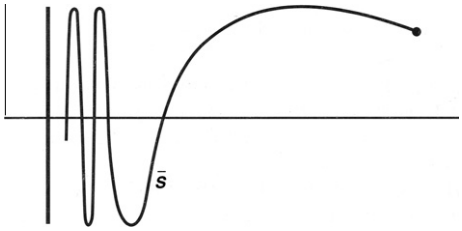

Fig. 1. Topologists sine curve from Example 1.

Since the inequality $\rho_A(p,q)+\rho_A(q,r)\geqslant\rho_A(p,r)-2\varepsilon$ holds for an arbitrary $\varepsilon>0$, we must also have $\rho_A(p,q)+\rho_A(q,r)\geqslant\rho_A(p,r)$, as required. □

Notice that for a constant function f_A we have $\rho_A\equiv 0$, so the property (ii) does not hold. In particular, in general, ρ_A is not a metric.

Now, consider the following alternative definition φ_A of the function ρ_A. In Theorem 1 we prove that under the very mild assumptions on the set D, which include all convex subsets of $\mathbb{R}^n$ (so, also, the rectangular regions), the mappings φ_A and ρ_A are identical. This gives a tool for approximating ρ_A in the digital space considered in Section 3.

Definition 3. Define the mapping $\varphi_A\colon D\times D\to[0,\infty)$ via formula

$$\varphi_A(p,q)=\inf_{\pi_1\in\Pi_{p,q}}\max_t f_A(\pi_1(t))-\sup_{\pi_0\in\Pi_{p,q}}\min_t f_A(\pi_0(t)).$$

Note that φ_A is defined by two separate paths. Also, as in the case of ρ_A, the minimum/maximum over numbers $t\in[0,1]$ exists, while neither infimum not supremum operators can be replaced by maximum/minimum.

Recall, that a set $D\subset\mathbb{R}^n$ is *simply connected*, provided it is path connected and for all $p,q\in D$ the paths $\pi_0,\pi_1\in\Pi_{p,q}$ are homotopic, that is, there exists a continuous function $h\colon[0,1]^2\to D$, known as a *homotopy* between π_0 and π_1, such that $h(\cdot,0)=\pi_0(\cdot)$, $h(\cdot,1)=\pi_1(\cdot)$, and $h(0,\cdot)$, $h(1,\cdot)$ constant. Intuitively, the homotopy condition means that D has no holes.

The proof of Theorem 1 will be based on the following two lemmas, the first of which is illustrated in Fig. 2.

Lemma 1. *Let F_0 and F_1 be a closed disjoint subsets of $[0,1]^2$ such that $F_0\setminus(0,1)^2\subset(0,1)\times\{1\}$ and $F_1\setminus(0,1)^2\subset(0,1)\times\{0\}$. Then, there exists a continuous path $\bar\pi:[0,1]\to[0,1]^2\setminus(F_0\cup F_1)$ from $\langle 0,.5\rangle$ to $\langle 1,.5\rangle$.*

Proof. The sets $\overline{F}_0=F_0\cup(\mathbb{R}\times[1,\infty))$ and $\overline{F}_1=F_1\cup(\mathbb{R}\times(-\infty,0])$ are disjoint and closed in $\mathbb{R}^2$. Moreover, there is a path from $\langle 0,.5\rangle$ to $\langle 1,.5\rangle$ both in $\mathbb{R}^2\setminus\overline{F}_0$ (following the lower boundary of $[0,1]^2$) and in $\mathbb{R}^2\setminus\overline{F}_1$ (following the upper boundary of $[0,1]^2$). Therefore, by a version of Alexander's lemma from [22, p. 137], there exists a path $\bar\pi_0:[0,1]\to\mathbb{R}^2\setminus(\overline{F}_0\cup\overline{F}_1)\subset\mathbb{R}\times(0,1)$ from $\langle 0,.5\rangle$ to $\langle 1,.5\rangle$. Now, if $r:\mathbb{R}\times(0,1)\to[0,1]\times(0,1)$ is such that $r(x)$ is the point in $[0,1]\times(0,1)$ closest to x, then the continuous mapping $\bar\pi=r\circ\bar\pi_0:[0,1]\to([0,1]\times(0,1))\setminus(F_0\cup F_1)$ is as desired. □

Lemma 2. *Let $D\subset\mathbb{R}^n$ be simply connected. For every $p,q\in D$ and $\varepsilon>0$ there exists a $\pi\in\Pi_{p,q}$ such that $U_0-\varepsilon<f_A(\pi(t))<U_1+\varepsilon$ for every $t\in[0,1]$, where $U_0=\sup_{\pi_0\in\Pi_{p,q}}\min_t f_A(\pi_0(t))$ and $U_1=\inf_{\pi_1\in\Pi_{p,q}}\max_t f_A(\pi_1(t))$.*

Proof. Choose the paths $\pi_0,\pi_1\in\Pi_{p,q}$ for which $\max_t f_A(\pi_1(t))<U_1+\varepsilon$ and $\min_t f_A(\pi_0(t))>U_0-\varepsilon$. Let $h\colon[0,1]^2\to D$ be a homotopy between the paths π_0 and π_1. Define $F_0=\{z\in[0,1]^2\colon f_A(h(z))\leqslant U_0-\varepsilon\}$ and $F_1=\{z\in[0,1]^2\colon f_A(h(z))\geqslant U_1+\varepsilon\}$ and notice that they satisfy the assumptions of Lemma 1. (Typical position of sets F_0 and F_1 is shown in Fig. 2. Function h is constant on each of the vertical segments of $[0,1]^2$.)

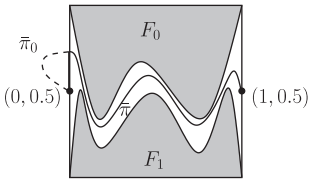

Fig. 2. Illustration of Lemma 1. See the text for notation.

Indeed, since functions $f_A\circ\pi_0$ and $f_A\circ\pi_1$ are continuous, the sets F_0 and F_1 are closed. They are disjoint, since $U_0-\varepsilon<f_A(p)=f_A(\pi_0(0,-_0-\varepsilon<f_A(p)=f_A(\pi_0(0,t))<U_1+\varepsilon$ for every $t\in[0,1]$. This inequality also implies that $F_0\cup F_1$ is disjoint with $\{0\}\times[0,1]$. Similarly, $F_0\cup F_1$ is disjoint with $\{1\}\times[0,1]$. Finally, F_0 is disjoint with $[0,1]\times\{0\}$, as for any point $z=\langle t,0\rangle\in[0,1]\times\{0\}$ we have $f_A(h(z))=f_A(\pi_0(t))>U_0-\varepsilon$, and F_1 is disjoint with $[0,1]\times\{1\}$, as $f_A(h(z))=f_A(\pi_1(t))<U_1+\varepsilon$ for every $t\in[0,1]$ and $z=\langle t,1\rangle\in[0,1]\times\{1\}$.

Since the assumptions of Lemma 1 are satisfied, there exists a continuous path $\bar\pi:[0,1]\to[0,1]^2\setminus(F_0\cup F_1)$ from $\langle 0,.5\rangle$ to $\langle 1,.5\rangle$. Then the path $\pi=h\circ\bar\pi:[0,1]\to D$ is as desired, since $\pi(0)=h(\bar\pi(0))=h(0,.5)=h(0,0)=\pi_0(0)=p$ and $\pi(1)=h(\bar\pi(1))=h(1,.5)=h(1,1)=\pi_1(1)=q$. Moreover, for every $t\in[0,1]$ we have $f_A(\pi(t))=f_A(h(\bar\pi(t)))\in(U_0-\varepsilon,U_1+\varepsilon)$, since otherwise $\bar\pi(t)$ is in $F_0\cup F_1$, contradicting the choice of $\bar\pi$. □

Theorem 1. *If $D\subset\mathbb{R}^n$ is simply connected, then the mappings ρ_A and φ_A are equal, that is, $\rho_A(p,q)=\varphi_A(p,q)$ for all $p,q\in D$.*

Proof. Fix $p,q\in D$ and an $\varepsilon>0$. It is enough to prove the following two inequalities: $\varphi_A(p,q)\leqslant\rho_A(p,q)+\varepsilon$ and $\rho_A(p,q)\leqslant\varphi_A(p,q)+2\varepsilon$. To prove the first of these, using the definition of ρ_A choose a $\pi\in\Pi_{p,q}$ for which $\rho_A(p,q)+\varepsilon\geqslant\tau_A(\pi)$. Then

$$\begin{aligned}\rho_A(p,q)+\varepsilon\geqslant\tau_A(\pi)&=\max_t f_A(\pi(t))-\min_t f_A(\pi(t))\\&\geqslant\inf_{\pi_1\in\Pi_{p,q}}\max_t f_A(\pi_1(t))-\sup_{\pi_0\in\Pi_{p,q}}\min_t f_A(\pi_0(t))=\varphi_A(p,q),\end{aligned}$$

giving the required inequality $\varphi_A(p,q)\leqslant\rho_A(p,q)+\varepsilon$.

To prove the second inequality, use Lemma 2 to find a path $\pi\in\Pi_{p,q}$ for which the range of $f_A\circ\pi$ is contained in $(U_0-\varepsilon,U_1+\varepsilon)$. Then

$$\rho_A(p,q)\leqslant\tau_A(\pi)\leqslant(U_1+\varepsilon)-(U_0-\varepsilon)=\varphi_A(p,q)+2\varepsilon,$$

finishing the proof. □

We will finish this section with a simple example of a continuous function $f_A\colon D\to[-1,1]$ defined on a path connected, not simple connected, subset D of $\mathbb{R}^2$ for which the conclusion of Theorem 1 does not hold.

Example 2. Let $D=\{\langle x,y\rangle\in\mathbb{R}^2:1\leqslant x^2+y^2\leqslant 4\}$, see Fig. 3, and let $f_A\colon D\to[-1,1]$ be defined via formula $f_A(x,y)=\frac{x}{\sqrt{x^2+y^2}}$. (This is the cosine function of the argument of $\langle x,y\rangle$.) Let $p=\langle 0,2\rangle$ and $q=\langle 0,-2\rangle$. Then, $\varphi_A(p,q)=0$, as $\varphi_A(p,q)\leqslant\max_t f_A(\pi_1(t))-\min_t f_A(-q\leqslant\nu\alpha\omega_t f_A\pi_1 t-\nu\iota\xi_t f_A\pi_0 t\varkappa\ \psi\theta\varepsilon\sigma\varepsilon\ \pi_1\in\Pi_{p,q}\ \iota\tau\ o\xi\ \upsilon\theta\varepsilon\ \mu\varepsilon\zeta\upsilon\ \theta\alpha\xi\delta\ \tau\iota\delta\varepsilon\ o\zeta\ \upsilon\theta\varepsilon\ \iota\xi\xi\varepsilon\sigma\ \gamma\iota\sigma\gamma\mu\varepsilon\ \alpha\xi\delta\ \pi_0\in\Pi_{p,q}\ \iota\tau\ \upsilon\theta\varepsilon\ \sigma\iota\eta\theta\upsilon\ \theta\alpha\xi\delta\ \tau\iota\delta\varepsilon\ o\zeta\ \upsilon\theta\iota\tau\ \gamma\iota\sigma\gamma\mu\varepsilon\varkappa\ \tau\varepsilon\varepsilon\ Z\iota\eta\varrho\ \varrho\ O\xi\ \upsilon\theta\varepsilon\ o\upsilon\theta\varepsilon\sigma\ \theta\alpha\xi\delta\varkappa\ \iota\upsilon\ \iota\tau\ \varepsilon\alpha\tau\ o\upsilon\ \tau\varepsilon\varepsilon\ \upsilon\theta\alpha\upsilon\ \rho_A p\varkappa q\ \varsigma\varrho$

3. The Minimum Barrier Distance in Z^n

In this section, we introduce a notion of the minimum barrier distance in digital setting, that is, for the bounded functions $\widehat{f}_A:\widehat{D}\to\mathbb{R}$, where $\widehat{D}$—a digital scene—is a finite subset of a digital space $\langle\phi\mathbb{Z}^n,\alpha\rangle$ defined as follows. $\mathbb{Z}$ is the set of integers, $\phi>0$ is a constant, $\phi\mathbb{Z}^n=\{\phi p:p\in\mathbb{Z}^n\}$, and α is an adjacency relation on $\phi\mathbb{Z}^n$. In what follows we will use the adjacency $\alpha=\alpha_1$, where for $\kappa\in\{1,\ldots,n-1\}$, two points in $\phi\mathbb{Z}^n$ are α_κ-adjacent provided at no coordinate they differ by more than ϕ and that the points differ in at most κ coordinates. Note that $\alpha=\alpha_1$ is equivalent to the standard 6-adjacency [23] in a 3D digital space; the theoretical formulations presented in the following is valid for α_κ for any other choice of κ, e.g., 18- or 26-adjacencies in 3D.

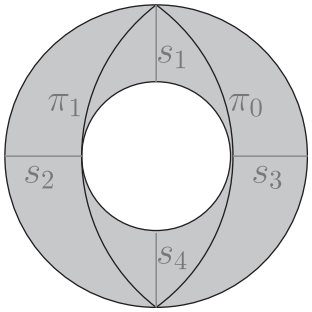

Fig. 3. The domain $D = \{\langle x,y\rangle \in \mathbb{R}^2 : 1 \leqslant x^2+y^2 \leqslant 4\}$ of $f_A(x,y) = \frac{x}{\sqrt{x^2+y^2}}$ and the paths π_0 and π_1 from Example 2. Note that f_A is constant on the segments s_1, s_2, s_3, s_4; it attains the values: 0 on s_1 and s_4, -1 on s_2, and 1 on s_3.

Recall, that a (digital) path in a subset $\widehat{D}$ of $\langle \phi\mathbb{Z}^n, \alpha\rangle$ is any ordered sequence $\hat{\pi} = \langle \hat{\pi}(0), \hat{\pi}(1), \ldots, \hat{\pi}(k)\rangle$ of points in $\widehat{D}$ such that $\hat{\pi}(i)$ is α-adjacent to $\hat{\pi}(i-1)$ for all $i \in \{1,2,\ldots,k\}$; the path $\hat{\pi}$ is from p to q when $\hat{\pi}(0) = p$ and $\hat{\pi}(k) = q$. For a fixed set $\widehat{D}$, a family of all paths in $\widehat{D}$ from p to q is denoted by $\widehat{\Pi}_{p,q}$ (or just $\widehat{\Pi}$, if p and q are clear from the context). Note that the digital paths are denoted by $\hat{\pi}$, while the paths in the continuous space $\mathbb{R}^n$ by π.

In what follows, we assume that the digital scenes $\widehat{D}$ are of the rectangular form $\widehat{D}_\phi = D \cap \phi\mathbb{Z}^n$, where $D = \{x \in \mathbb{R}^n : L_i \leqslant x(i) \leqslant U_i\}$ for some real numbers L_i, U_i such that $L_i < U_i$ for all i. In particular, any two points in $\widehat{D}$ are connected by a path.

In view of Theorem 1, there are two natural ways of defining the discrete minimum barrier distance for $\widehat{f_A} : \widehat{D} \to \mathbb{R}$, the discretization of the formulas for $\rho_A(p,q)$ and for $\varphi_A(p,q)$:

$$\widehat{\rho_A}(p,q) = \min_{\hat{\pi}\in\widehat{\Pi}_{p,q}} \left(\max_i [\widehat{f_A}(\hat{\pi}(i))] - \min_j [\widehat{f_A}(\hat{\pi}(j))]\right), \tag{3}$$

$$\widehat{\varphi_A}(p,q) = \min_{\hat{\pi}_1\in\widehat{\Pi}_{p,q}} \max_i [\widehat{f_A}(\hat{\pi}_1(i))] - \max_{\hat{\pi}_0\in\widehat{\Pi}_{p,q}} \min_j [\widehat{f_A}(\hat{\pi}_0(j))]. \tag{4}$$

3.1. Properties of $\widehat{\rho_A}$ and $\widehat{\varphi_A}$

Proposition 2.

(i) *Each of the functions $\widehat{\rho_A}$ and $\widehat{\varphi_A}$ is a pseudo-metric on $\widehat{D}$.*
(ii) *$\widehat{\varphi_A}(p,q) \leqslant \widehat{\rho_A}(p,q)$ for all $p,q \in \widehat{D}$. The equality need not hold.*
(iii) *The paths cost functions $\max_i[\widehat{f_A}(\hat{\pi}_1(i))]$ and $\min_j[\widehat{f_A}(\hat{\pi}_0(j))]$ are smooth in the sense of [16]. So, the transform $\widehat{\varphi_A}(p,\cdot)$ can be efficiently calculated by Dijkstra's algorithm. However, the path cost function $\max_i[\widehat{f_A}(\hat{\pi}(i))] - \min_j[\widehat{f_A}(\hat{\pi}(j))]$ is not smooth in the sense of [16] and effective computing of the transform $\widehat{\rho_A}(p,\cdot)$ presents a challenge.*

Proof. The proof of (i) is an easier version of that for Proposition 1.

To see (ii), choose $\hat{\pi}$ with $\widehat{\rho_A}(p,q) = \max_i[\widehat{f_A}(\hat{\pi}(i))] - \min_j[\widehat{f_A}(\hat{\pi}(j))]$. Then the inequalities $\min_{\hat{\pi}_1\in\widehat{\Pi}_{p,q}} \max_i[\widehat{f_A}(\hat{\pi}_1(i))] \leqslant \max_i[\widehat{f_A}(\hat{\pi}(i))]$ and $\max_{\hat{\pi}_0\in\widehat{\Pi}_{p,q}} \min_j[\widehat{f_A}(\hat{\pi}_0(j))] \geqslant \min_j[\widehat{f_A}(\hat{\pi}(j))]$ imply

$$\widehat{\varphi_A}(p,q) \leqslant \max_i[\widehat{f_A}(\hat{\pi}(i))] - \min_j[\widehat{f_A}(\hat{\pi}(j))] = \widehat{\rho_A}(p,q).$$

An example that equality need not hold can be found in Fig. 4.

(iii) Smoothness of the path cost functions for $\widehat{\varphi_A}(p,q)$ is easy to check and well known. (This was proved, for example, in [16].) Lack of such smoothness for $\widehat{\rho_A}(p,q)$ can be seen in Fig. 4: There is a unique $\widehat{\rho_A}$-optimal path from the seed point to the upper right element, but its restriction to the first three elements is not $\widehat{\rho_A}$-optimal. □

Next we will prove, in Theorem 2, that if $\widehat{f_A} : \widehat{D}_\theta \to \mathbb{R}$ is a discretization of a continuous function f_A defined on a rectangular region D, then, for a sufficiently small ϕ, the numbers $\widehat{\varphi_A}(p,q)$ and $\widehat{\rho_A}(p,q)$ well approximate $\varphi_A(p,q) = \rho_A(p,q)$. Of course, in practice we do not have continuous images $f_A : D \to \mathbb{R}$, but the assumption is reasonable since most image acquisition methods induce smoothing of the image scene by a point spread function, see for example [24] for a discussion. Such an f_A can also be found by an interpolation of a digital function (often, just an image intensity function). We used this approach in our experiments presented in the next section.

In the proof of Theorem 2 we will need the following notion. The *hypervoxel* of a point p in $\phi\mathbb{Z}^n$ is the Voronoi region of p in $\mathbb{R}^n$, that is, the set $\{x \in \mathbb{R}^n : |x(i) - p(i)| \leqslant \phi/2 \text{ for all } i\}$. The *supercover digitization* in $\phi\mathbb{Z}^n$ of a subset A of $\mathbb{R}^n$, denoted $\mathcal{S}(A)$, is the union of all hypervoxels that meet the set A. The following simple fact can be found, for example, in [25]. (Compare also [20].)

Remark 2. The supercover of any continuous path π in the rectangular region $D \subset \mathbb{R}^n$ (or, more precisely, of its image $\pi[0,1] = \{\pi(t): t \in [0,1]\}$) induces, in $\widehat{D}_\phi = D \cap \phi\mathbb{Z}^n$, an α-adjacent path $\hat{\pi} = \langle \hat{\pi}(0), \hat{\pi}(1), \ldots, \hat{\pi}(k)\rangle$ with $\pi[0,1] \subset \mathcal{S}(\{\hat{\pi}(0), \hat{\pi}(1), \ldots, \hat{\pi}(k)\})$ and $\{\hat{\pi}(0), \hat{\pi}(1), \ldots, \hat{\pi}(k)\} \subset \mathcal{S}(\pi[0,1])$. In particular, the Hausdorff distance between the sets $\{\hat{\pi}(0), \hat{\pi}(1), \ldots, \hat{\pi}(k)\}$ and $\pi[0,1]$ is at most $\phi\sqrt{n}/2$, that is,

- for every i there is a t with $\|\hat{\pi}(i) - \pi(t)\| \leqslant \phi\sqrt{n}/2$ and, similarly, for every t there is an i with $\|\hat{\pi}(i) - \pi(t)\| \leqslant \phi\sqrt{n}/2$.

Theorem 2. *Let D be a rectangular region in $\mathbb{R}^n$ and $f_A : D \to \mathbb{R}$ be continuous. Let $\widehat{\rho_A}$ and $\widehat{\varphi_A}$ be the discrete minimum barrier distance functions for the sampling $\widehat{f_A}$ of f_A on $\widehat{D}_\phi$, that is, with $\widehat{f_A}(p) = f_A(p)$ for all $p \in \widehat{D}_\phi$. Then, for every $\varepsilon > 0$ there exists a $\phi_0 > 0$ such that for every $\phi \in (0, \phi_0]$*

(•) $|\widehat{\rho_A}(p,q) - \rho_A(p,q)| < \varepsilon$ and $|\widehat{\varphi_A}(p,q) - \varphi_A(p,q)| < \varepsilon$ for all $p,q \in \widehat{D}_\phi$.

More precisely, this holds for any $\phi_0 > 0$ such that $|f_A(x) - f_A(y)| < \varepsilon/4$ for any $x,y \in D$ with $\|x - y\| \leqslant \phi_0\sqrt{n}/2$.

Proof. Since D is compact and f_A is continuous, f_A is uniformly continuous. So, there exists a $\phi_0 > 0$ from the last sentence of the theorem. We need to show that (•) holds for such a ϕ_0. We will show this only for the operator ρ_A, the argument for the operator φ_A being similar.

To show this, fix $p,q \in \widehat{D}_\phi$. We need to prove that $\widehat{\rho_A}(p,q) < \rho_A(p,q) + \varepsilon$ and $\rho_A(p,q) < \widehat{\rho_A}(p,q) + \varepsilon$. To argue for the first of these inequalities, choose a $\pi \in \Pi_{p,q}$ for which $\max_t f_A(\pi(t)) - \min_t f_A(\pi(t)) < \rho_A(p,q) + \varepsilon/2$. Let $\hat{\pi}$ be as in Remark 2 and let i_0 be such that $\max_i[\widehat{f_A}(\hat{\pi}(i))] = f_A(\hat{\pi}(i_0))$. Then, there is a t_0 for which $\|\pi(t_0) - \hat{\pi}(i_0)\| \leqslant \phi_0\sqrt{n}/2$. So, $|f_A(\pi(t_0)) - f_A(\hat{\pi}(i_0))| \leqslant \varepsilon/4$ and $\max_i[\widehat{f_A}(\hat{\pi}(i))] = f_A(\hat{\pi}(i_0)) \leqslant f_A(\pi(t_0)) + \varepsilon/4 \leqslant \max_t[f_A(\pi(t))] + \varepsilon/4$. Similarly, we prove that $\min_i[\widehat{f_A}(\hat{\pi}(i))] \geqslant \min_t[f_A(\pi(t))] - \varepsilon/4$. Hence

$$\begin{aligned}\widehat{\rho_A}(p,q) &\leqslant \max_i[\widehat{f_A}(\hat{\pi}(i))] - \min_j[\widehat{f_A}(\hat{\pi}(j))] \\ &\leqslant \max_t f_A(\pi(t)) - \min_t f_A(\pi(t)) + \varepsilon/2 < \rho_A(p,q) + \varepsilon/2 + \varepsilon/2,\end{aligned}$$

proving $\widehat{\rho}_A(p,q) < \rho_A(p,q) + \varepsilon$. The inequality $\rho_A(p,q) < \widehat{\rho}_A(p,q) + \varepsilon$ is proved similarly. □

Since, by Theorem 2, both $\widehat{\rho_A}(p,q)$ and $\widehat{\varphi_A}(p,q)$ converge, as $\phi \to 0$, to $\rho_A(p,q) = \varphi_A(p,q)$, we obtain the following corollary.

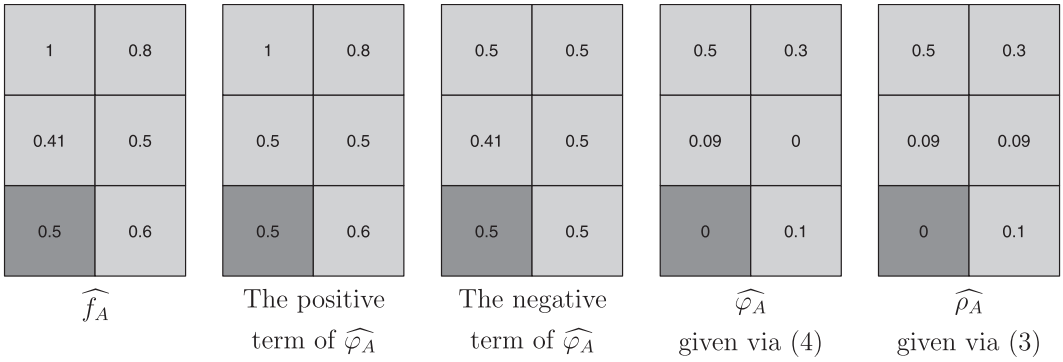

Fig. 4. Values of $\widehat{\rho_A}$ and $\widehat{\varphi_A}$ obtained on a small image. Note the difference between $\widehat{\rho_A}$ and its approximation $\widehat{\varphi_A}$. The dark gray pixel corresponds to the point with respect to which the path values are calculated.

Corollary 1. $\max_{p,q\in\widehat{D}_\phi} |\widehat{\rho_A}(p,q) - \widehat{\varphi_A}(p,q)| \to 0$ *as* $\phi \to 0$.

3.2. The algorithm

Among the two versions of the discrete minimum barrier distance functions, $\widehat{\rho_A}(p,q)$ and $\widehat{\varphi_A}(p,q)$, only the first one is defined as the minimal (appropriately defined) length of a single path from p to q—the feature shared by essentially all useful distance notions. Because of this property, it is the function $\widehat{\rho_A}$, rather than $\widehat{\varphi_A}$, that we consider to be the proper definition of the discrete minimum barrier distance. So, why did we not stick in this paper to the discussion $\widehat{\rho_A}$ (and bothered with $\widehat{\varphi_A}$, φ_A, and ρ_A)?

An answer is given by Proposition 2(iii): there seems to be no algorithm that efficiently computes the exact value of $\widehat{\rho_A}(p,q)$. To solve this predicament, we turned to finding an efficient algorithm for finding an approximation of $\widehat{\rho_A}$. According to Corollary 1, which combines Theorems 1 and 2, the function $\widehat{\varphi_A}$ constitutes an approximation of $\widehat{\rho_A}$. Moreover, $\widehat{\varphi_A}(p,\cdot)$ can be found by a Dijkstra's algorithm, which computes each of the terms $\min_{\widehat{\pi}_1\in\widehat{\Pi}_{p,q}} \max_i[\widehat{f_A}(\widehat{\pi}_1(i))]$ and $\max_{\widehat{\pi}_0\in\widehat{\Pi}_{p,q}} \min_j[\widehat{f_A}(\widehat{\pi}_0(j))]$ separately. In particular, the time complexity of such algorithm is $O(N\log N)$, where N is the number of points in the image domain. In what follows, we will use the output of this algorithm as an approximation of $\widehat{\rho_A}$.

It is worth to mention, that there are other algorithms with the same computational complexity, that approximate $\widehat{\rho_A}$. For example, in [21], an approximation of $\widehat{\rho_A}$ (for vectorial functions $\widehat{f_A}$) is found by a version of Dijkstra's algorithm, which propagates according to the path cost function $\max_i[\widehat{f_A}(\widehat{\pi}(i))] - \min_j[\widehat{f_A}(\widehat{\pi}(j))]$. A similar approach was used in a preliminary version of this paper. The experimental results show that the output of such algorithm is very close to $\widehat{\varphi_A}$ (so, it approximates $\widehat{\rho_A}$). However, at the present time, there is no theoretical result (in form of Corollary 1) that the output of such algorithm must approximate $\widehat{\rho_A}$. Thus, so far, $\widehat{\varphi_A}$ constitutes the best approximation of $\widehat{\rho_A}$.

4. The experiments

In this section, we compare the minimum barrier distance $\widehat{\varphi_A}$, approximating $\widehat{\rho_A}$, with the following distance functions, described in detail below: fuzzy distance d_F, geodesic distance d_G, and max-arc distance $d_{\max}$. Having in mind the applicability of the distance functions in image segmentations, we will concentrate on examining two desired properties that a distance function should have: (A) producing the high ratios between the inter-object distances and the intra-object distances; (B) being relatively unaffected by a change of the position of seeds (robustness with respect seeds position) and by an introduction of noise and blur to the image intensity function. Therefore, our experiments are designed to measure how each of these distances is influenced by a change of the position of seeds, Fig. 5, and an introduction of noise and blur to the image intensity function, Figs. 6 and 7. Notice, that the study of noise and blur effects give, in particular, an information of the ratio from (A). All distances we consider ($\widehat{\varphi_A}$, d_F, d_G, and $d_{\max}$) are computed by minor variations of Dijkstra wave-front propagation algorithm. So, the time complexity of each of these algorithms is $O(N\log N)$, where N is the number of points in the image domain.

For each of the distance measures d_F, d_G, and $d_{\max}$, the distance between two points, p and q, is defined as the minimal cost of a path between p and q, where the cost of a path $\langle p_1, p_2, \ldots, p_m\rangle$ is defined as follows:

- For the *fuzzy distance*,

$$\sum_{i=1}^{m-1} \frac{f_A(p_i) + f_A(p_{i+1})}{2} \cdot \|p_i - p_{i+1}\|.$$

See [5,15] for more details. We will also consider the *fuzzy distance on edge* image, where the fuzzy distance is instead applied to an edge image obtained by extracting edges of the image by an edge detection filter. Here, we use gradient magnitude obtained by the Prewitt operator.

- For the geodesic distance d_G

$$\sum_{i=1}^{m-1} \omega|f_A(p_i) - f_A(p_{i+1})| + \|p_i - p_{i+1}\|. \tag{5}$$

See [15,26] for details. The parameter ω affects trade-off between the fuzzy membership values and the distance on the image scene.[1]

- For the *max-arc* distance $D_{\max}$

$$\max_{i=1,\ldots,m-1} \psi(f_A(p_i), f_A(p_{i+1})),$$

where ψ is a function that measures dissimilarity between points in the image. Here, we use $\psi(f_A(p_i), f_A(p_{i+1})) = |f_A(p_i) - f_A(p_{i+1})|$. See [16] for details. The max-arc distance can be seen as a reverse (with respect to the order) of fuzzy connectedness measure with the affinity function ψ. (See e.g. [17,18,20].)

4.1. The results

In all experiments we use 2D images considered with the 4-connectedness (α-adjacency). Note that all algorithms are "blind" in the sense that no prior information is considered. Fuzzy connected-

[1] Formula (5) can be also expressed as $\sum_{i=1}^{n-1} \mathrm{dist}(\langle p_i, \omega f_A(p_i)\rangle, \langle p_{i+1}, \omega f_A(p_{i+1})\rangle)$, where dist is the taxicab metric, that is, $\mathrm{dist}(\langle x_1, y_1\rangle, \langle x_2, y_1\rangle) = \|x_1 - x_2\| + \|y_1 - y_2\|$. In standard analysis courses, the geodesic distance is usually defined with the standard Euclidean distance $\sqrt{\|x_1 - x_2\|^2 + \|y_1 - y_2\|^2}$.

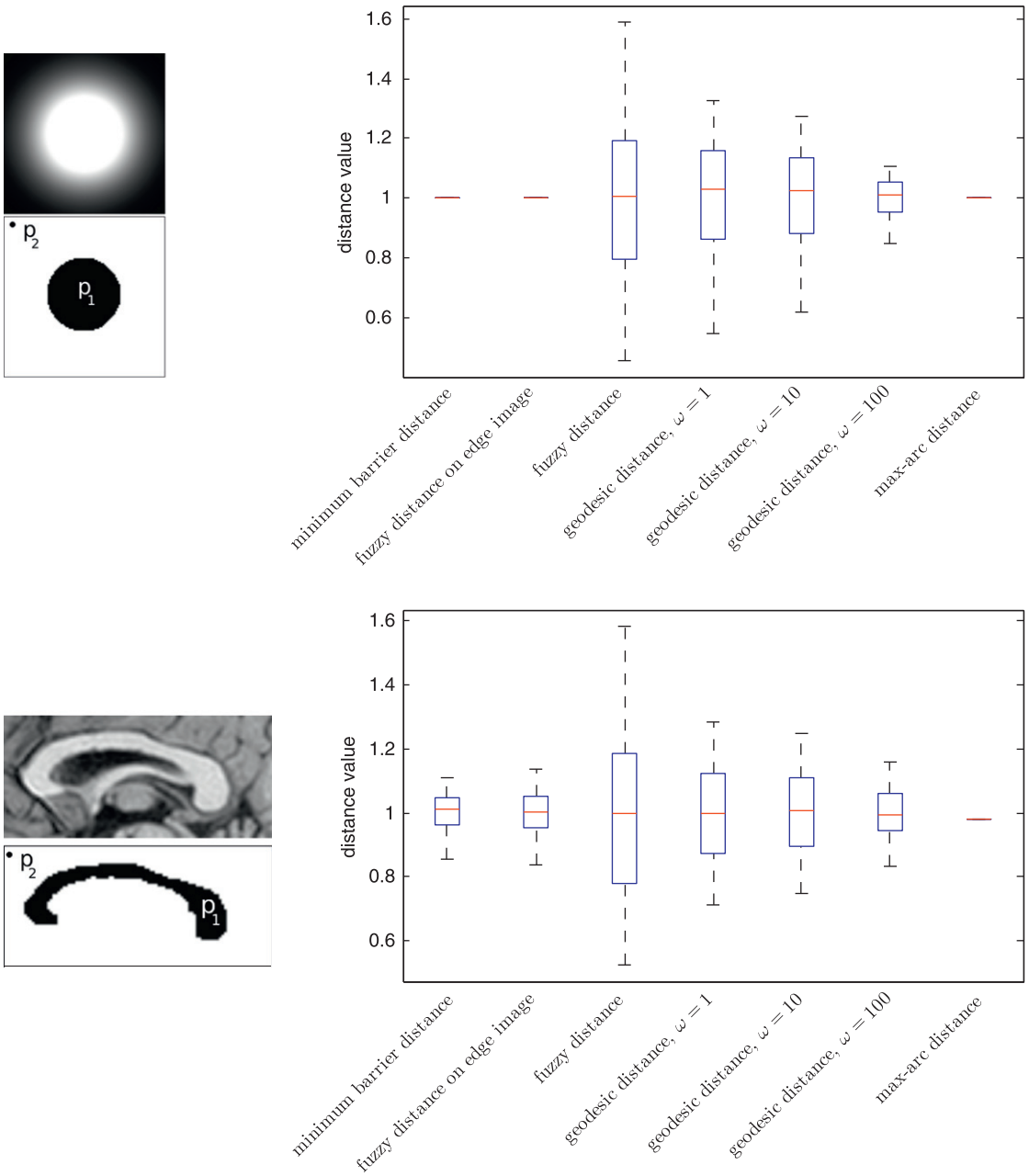

Fig. 5. Stability of the distance values $d(p_1,p_2)$ for different distance functions, where the external seed point p_2 is fixed and the internal seed point p_1 is chosen randomly, within the black region indicated on the left. The distance values are normalized, so that the mean distance value is one. The boxes in the boxplots cover the 25th to the 75th percentile and central mark is the median. The whiskers of the boxplots extend to the most extreme data points not considered outliers.

ness (and therefore max-arc distance), for example, can incorporate an object feature based component with prior information about for example the expected intensity in an object, see [17,18]. Including such features would require training.

4.1.1. Stability with respect to the seed points position

To test the different distance functions for its stability with respect to the change of the seed points position, we use two test images presented in each row of Fig. 5 as the top image of the left column. The boxplots in Fig. 5 show, for each distance function, the distribution of the distance value between a fixed (external) seed point p_2 and, for each of the 1000 repetitions of the experiment, an internal seed point p_1 randomly chosen within the black region indicated on the left of the figure.

4.1.2. Stability with respect to noise and smoothing (blur)

The results of the experiments are presented, respectively, in Figs. 6 and 7. The original tested images are shown at the top of the figures. In the noise experiment, the images are degraded by an additive Gaussian noise with zero mean and variance values of: 0.0001, 0.001, 0.01, 0.1 and 1. For the blur experiment, we use Gaussian smoothing with σ between 0 and 3. The setup is as follows: two inter-object seeds, p_1 and p_2, and an intra-object seed p_3 are fixed for the entire experiment; (i) Gaussian noise is randomly generated 1000 times for each value of σ; and (ii) the image is filtered with a Gaussian filter with different values of σ. In each iteration, we calculate the inter-object distance between p_1 and p_2, as well as the intra-object distance between p_1 and p_3. The distance values are scaled so that the distance between p_1 and p_3 is 1 on the original image. The figures show, for each distance function and

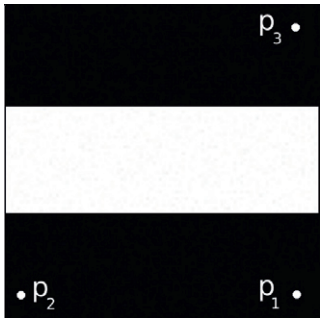

Test image (f_A).

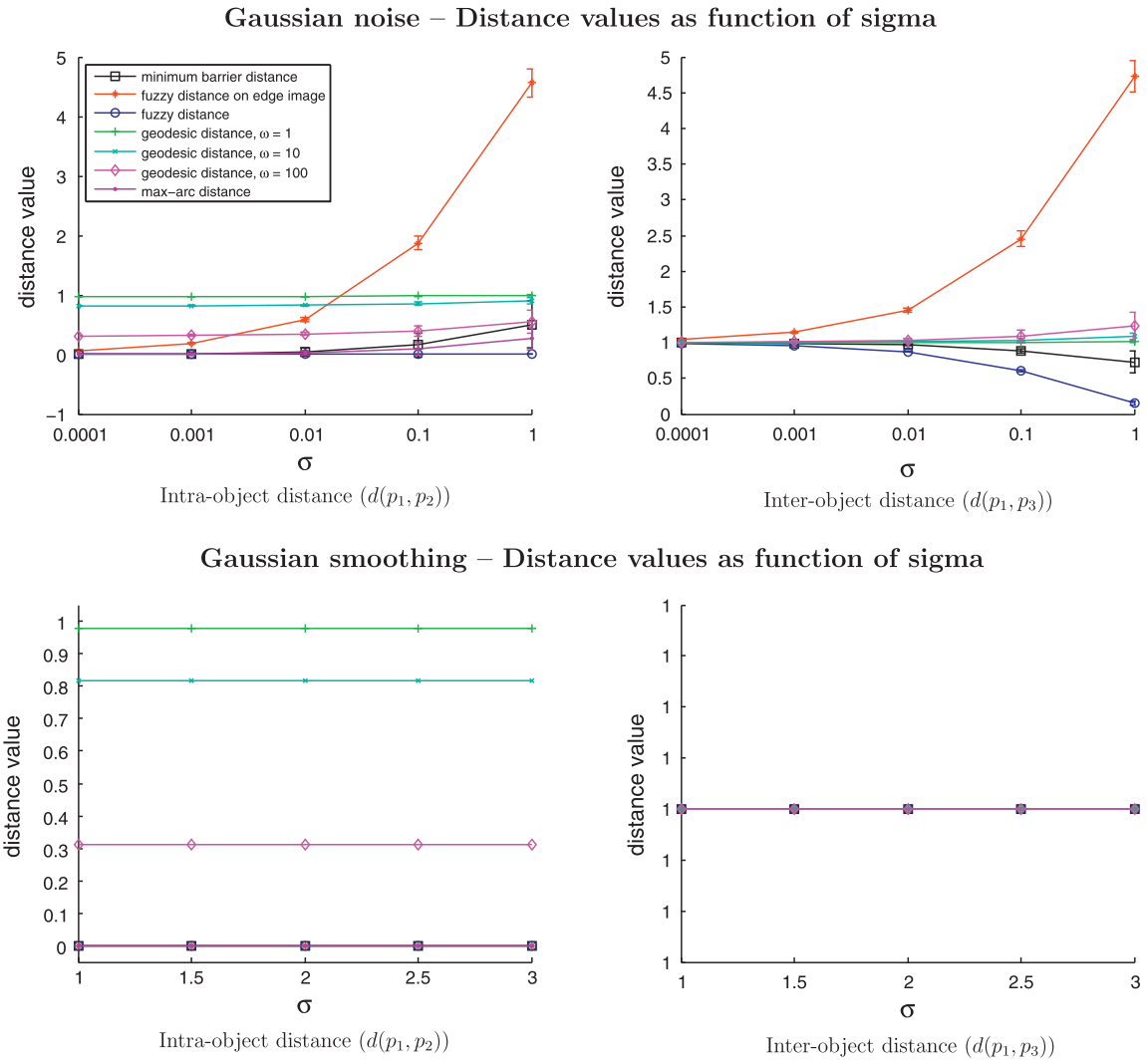

Fig. 6. Stability to Gaussian noise and smoothing, see the text. The distance values are normalized so that $d(p_1,p_3) = 1$ on the original image. The confidence intervals in the upper plots cover one standard deviation.

each distortion, the median of the obtained values as well as the associated confidence interval.

4.2. Interpretation of the experimental results

According to Fig. 5, the max-arc distance $d_{\max}$ is by far the most robust with respect to seed choice. This is not surprising, since according to the seed-robustness theorem for fuzzy connectedness, changing a seed p_1 to another seed p_1' within the same fuzzy connectedness object (defined via $d_{\max}$) does not affect at all the delineated object. The strong point for the minimum barrier distance is that, from this point of view, the minimum barrier distance is only a bit worst than $d_{\max}$ and far better than other distances we consider.

The experiments also verify, see Figs. 6 and 7, that the minimum barrier distance has, in general, low sensitivity to noise and blur. At the same time, the distances based on gradient magnitude (fuzzy distance on edge image and max-arc distance) are sensitive to noise, see Fig. 7. In particular, while the max-arc distance $g_{\max}$ is stable when strong gradients are present, the inter-object $g_{\max}$ distance is not stable against Gaussian smoothing, as can be seen in Fig. 7.

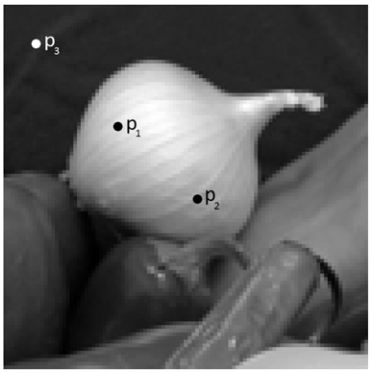

Test image (f_A).

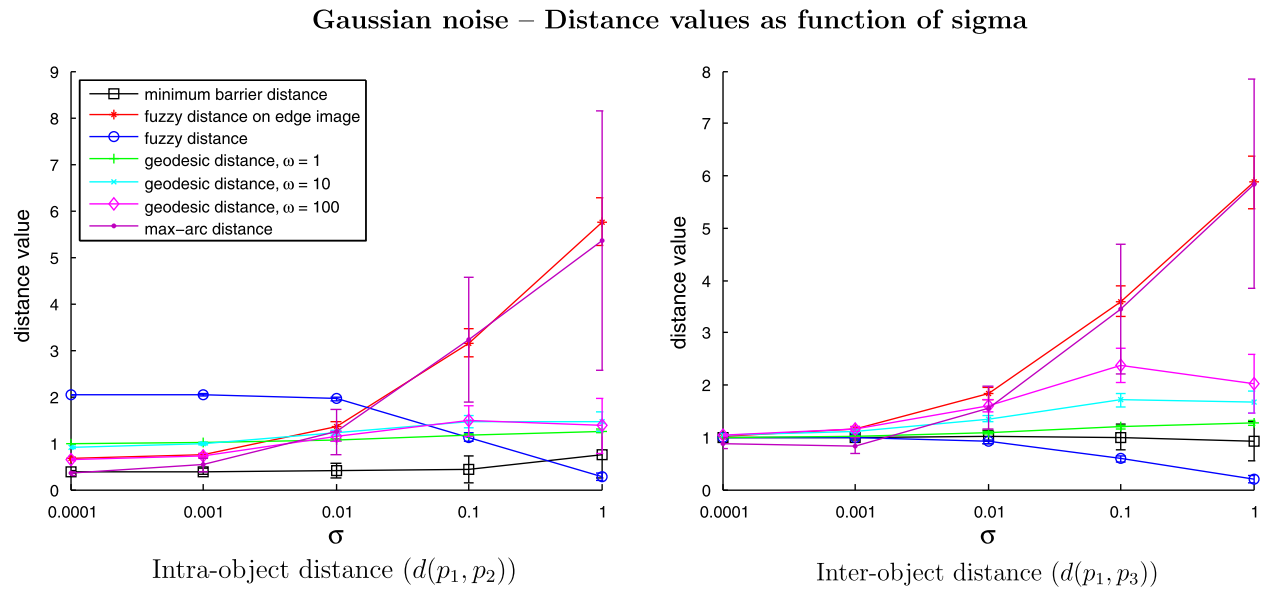

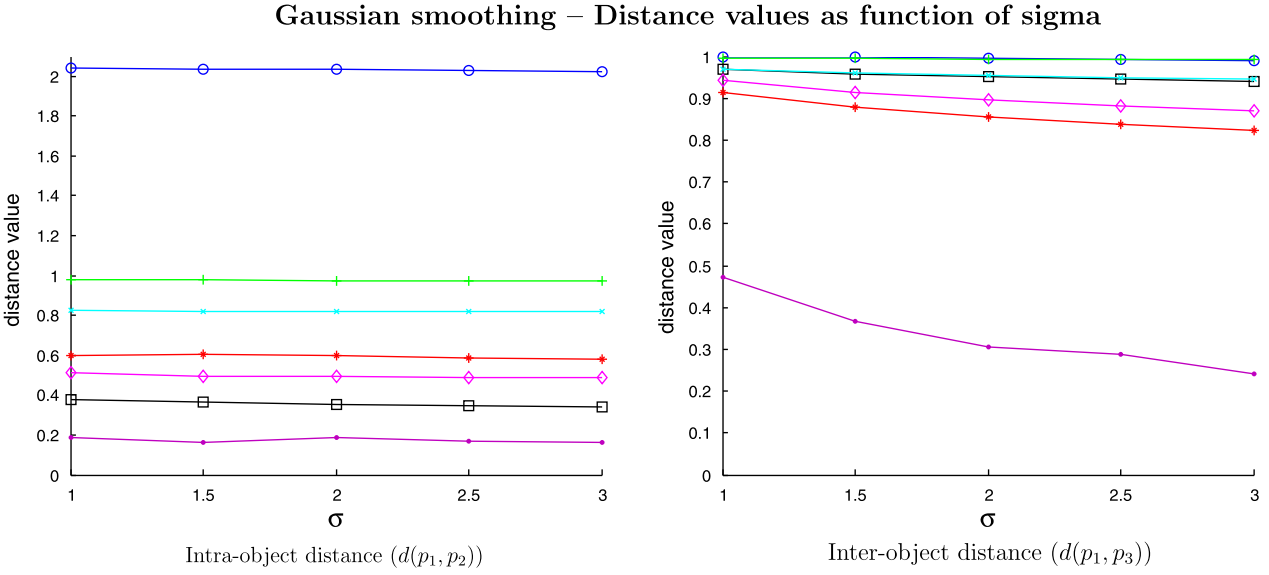

Fig. 7. Stability to Gaussian noise and smoothing, see the text. The distance values are normalized so that $d(p_1, p_3) = 1$ on the original image. The confidence intervals in the upper plots cover one standard deviation.

The positive exception here is the fuzzy distance function, which performs well on the intensity image when the intensities within an object are low and the intensities between different objects are high. This can be seen in Fig. 6, where the intensities within an object are low and the intensities between different objects are high, and in Fig. 7, where the intensities within the object are

high, which results in a high intra-object distance and a low inter-object distance. (The weak performance of the fuzzy distance function is its dependence on seed position, see above.)

Finally, notice in Figs. 6 and 7, that all considered distances perform reasonably well in separating the object and background, in the sense described in (A) above. However, as seen in Fig. 5, the performance of the max-arc distance $g_{\max}$ is considerably better for the images with the strong gradient and no noise (Fig. 6) than when the gradients are weak as in Fig. 7. There is no similar drop of performance with this respect for the minimum barrier distance.

In summary, the minimum barrier distance function compares favorable with the other distances we compared it with. This make it a good candidate for many many imaging tasks, that use distance functions.

5. Conclusions and future work

In this paper we proposed a novel distance function, the minimum barrier distance, which effectively computes the distance values for digital images. It compares favorable with the fuzzy, geodesic, and max-arc distances, when considered is stability with respect to change of seed position and introduction of noice or blur.

The main characteristic of the value of minimum barrier distance is based on the image homogeneity, making it robust against weak gradients and noise. This stays in contrast with many other distance functions, used in the wave-front propagation segmentation methods (like watersheds [27,28] and fuzzy connectedness [17,18]), which are based on gradient information, image inhomogeneity, and so are less robust for noise and do not perform well for the images with weak gradients.

In the geodesic distance, the parameter ω in (5) gives the trade-off between the accumulated gradient magnitude along the path and the accumulated Euclidean distance between consecutive points. High ω gives low robustness to noise and low ω gives a distance function that is independent of the intensities.

Notice that the computational complexity for finding the approximation of the minimum barrier distance $\widehat{\varphi}$ is low, since the standard Dijkstra wave-front propagation algorithms can be used. However, to approximate with higher accuracy and precision, we need to increase the resolution. If we need to better approximate ρ, this could mean a substantial increase in computational complexity. We note that subsampling is not needed in homogenous regions.

In our future work, we plan to make local approximations in regions where the inhomogeneity of f_A is high. In this way we think that we will achieve better approximation without significant increase in computational complexity. We also plan to examine the case with multiple seed points in our future work.

We believe that this method has the potential of being useful in many applications where homogeneous regions are extracted, for example segmentation.

Acknowledgment

We thank the anonymous reviewers for their insightful comments that helped us to improve this manuscript.

References

[1] A. Rosenfeld, J.L. Pfaltz, Distance functions on digital pictures, Pattern Recog. 1 (1968) 33–61.
[2] G. Borgefors, Distance transformations in arbitrary dimensions, Comput. Vis. Graph. Image Process. 27 (1984) 321–345.
[3] G. Borgefors, On digital distance transforms in three dimensions, Comput. Vis. Image Understand. 64 (3) (1996) 368–376.
[4] P.-E. Danielsson, Euclidean distance mapping, Comput. Graph. Image Process. 14 (1980) 227–248.
[5] P.K. Saha, F.W. Wehrli, B.R. Gomberg, Fuzzy distance transform: theory, algorithms, and applications, Comput. Vis. Image Understand. 86 (2002) 171–190.
[6] R. Strand, Distance Functions and Image Processing on Point-Lattices: With Focus on the 3D Face- and Body-Centered Cubic Grids, Ph.D. Thesis, Uppsala University, Sweden, 2008. <http://urn.kb.se/resolve?urn=urn:nbn:se:uu:diva-9312>.
[7] R. Strand, B. Nagy, G. Borgefors, Digital distance functions on three-dimensional grids, Theor. Comput. Sci. 412 (15) (2011) 1350–1363.
[8] T. Hildebrand, P. Rüegsegger, A new method for the model-independent assessment of thickness in three-dimensional images, J. Microsc. 185 (1) (1997) 67–75.
[9] P.K. Saha, Z. Gao, S.K. Alford, M. Sonka, E.A. Hoffman, Topomorphologic separation of fused isointensity objects via multiscale opening: separating arteries and veins in 3-D pulmonary CT, IEEE Trans. Med. Imag. 29 (3) (2010) 840–851.
[10] P.K. Saha, F.W. Wehrli, Measurement of trabecular bone thickness in the limited resolution regime of in vivo MRI by fuzzy distance transform, IEEE Trans. Med. Imag. 23 (1) (2004) 53–62.
[11] A. Rosenfeld, J.L. Pfaltz, Sequential operations in digital picture processing, J. ACM 13 (4) (1966) 471–494.
[12] C.R. Maurer Jr., R. Qi, V. Raghavan, A linear time algorithm for computing exact Euclidean distance transforms of binary images in arbitrary dimensions, IEEE Trans. Pattern Anal. Mach. Intell. 25 (2) (2003) 265–270.
[13] K.C. Ciesielski, X. Chen, J.K. Udupa, G.J. Grevera, Linear time algorithm for exact distance transform, J. Math. Imag. Vis. 39 (3) (2011) 193–209.
[14] J.A. Sethian, Level Set Methods and Fast Marching Methods, Cambridge University Press, 1999.
[15] C. Fouard, M. Gedda, An objective comparison between gray weighted distance transforms and weighted distance transforms on curved spaces, in: A. Kuba, L.G. Nyúl, K. Palágyi (Eds.), Discrete Geometry for Computer Imagery, 13th International Conference, DGCI 2006, Szeged, Hungary, October 25–27, 2006, Proceedings Lecture Notes in Computer Science, vol. 4245, Springer, 2006, pp. 259–270.
[16] A.X. Falcão, J. Stolfi, R. de Alencar Lotufo, The image foresting transform: theory, algorithms, and applications, IEEE Trans. Pattern Anal. Mach. Intell. 26 (1) (2004) 19–29.
[17] J.K. Udupa, P.K. Saha, R.A. Lotufo, Relative fuzzy connectedness and object definition: theory, algorithms, and applications in image segmentation, IEEE Trans. Pattern Anal. Mach. Intell. 24 (2002) 1485–1500.
[18] J.K. Udupa, P.K. Saha, Fuzzy connectedness and image segmentation, Proc. IEEE 91 (10) (2003) 1649–1669.
[19] A. Rosenfeld, Fuzzy digital topology, Inform. Control 40 (1) (1979) 76–87.
[20] K.C. Ciesielski, J.K. Udupa, A framework for comparing different image segmentation methods and its use in studying equivalences between level set and fuzzy connectedness frameworks, Comput. Vis. Image Understand. 115 (6) (2011) 721–734.
[21] A. Kårsnäs, R. Strand, P.K. Saha, The vectorial minimum barrier distance, in: Proceedings of the 21st International Conference on Pattern Recognition, November 2012, Japan, pp. 792–795.
[22] M.H.A. Newman, Elements of the Topology of Plane Sets of Points, Cambridge, 1964.
[23] T.Y. Kong, A. Rosenfeld, Digital topology: introduction and survey, Comput. Vis. Graph. Image Process. 48 (3) (1989) 357–393.
[24] U. Köthe, What can we learn from discrete images about the continuous world? in: D. Coeurjolly, I. Sivignon, L. Tougne, F. Dupont (Eds.), Discrete Geometry for Computer Imagery, 14th International Conference, DGCI 2008, Lyon, France, 2008, Proceedings, Lecture Notes in Computer Science, vol. 4992, Springer, 2008, pp. 4–19.
[25] P. Stelldinger, Topologically correct 3D surface reconstruction and segmentation from noisy samples, in: V. Brimkov, R. Barneva, H. Hauptman (Eds.), Proceedings of the 12th International Conference on Combinatorial Image Analysis, Lecture Notes in Computer Science, vol. 4958, Springer-Verlag, Berlin, Heidelberg, 2008, pp. 274–285.
[26] P.J. Toivanen, New geodesic distance transforms for gray-scale images, Pattern Recog. Lett. 17 (1996) 437–450.
[27] L. Vincent, P. Soille, Watersheds in digital spaces: an efficient algorithm based on immersion simulations, IEEE Trans. Pattern Anal. Mach. Intell. 13 (6) (1991) 583–598.
[28] P. Soille, Morphological Image Analysis: Principles and Applications, second ed., Springer-Verlag, New York, Inc., Secaucus, NJ, USA, 2003.